International Journal of Heat and Technology
Vol. 41, No. 3, June, 2023, pp. 529-540
Journal homepage: http://iieta.org/journals/ijht

Heat Transfer Characteristics on MHD Oscillatory Radiative Nanofluid with $H_2O/C_2H_6O_2$ (Basefluid): A Comparative Study of Different Nanoparticles of Various Shapes

Jaismitha Barkilean, Sasikumar Jagadeesan*

Department of Mathematics, Faculty of Engineering and Technology, SRM Institute of Science and Technology, Kattankulathur 603203, Tamil Nadu, India

Corresponding Author Email: sasikumj@srmist.edu.in

https://doi.org/10.18280/ijht.410305

Received: 1 March 2023
Accepted: 16 June 2023

Keywords:
thermal radiation, MHD, oscillatory flow, heat transfer, nanofluid flow, porous medium

ABSTRACT

The reviews in the literature reveal that nanofluids are more efficient for heat transfer than regular base fluids. The liquids that contain suspended nanoparticles have gained significant attention in recent years due to their potential enhancement of heat transfer in various applications including electronics cooling, power generation, and refrigeration. The present research work aims to examine the MHD radiative oscillatory nanofluid flow in a porous medium through an asymmetric wavy channel. The partial differential equations with physical boundary conditions represent the mathematical model of the flow problem. The governing equations are solved by the analytical method. H_2O-Water and $C_2H_6O_2$-ethylene glycol (EG) as base fluids are used with four different types of nanoparticles, namely gold (Au), copper (Cu), alumina (Al_2O_3), and silver (Ag). Graphs for velocity and temperature profiles are drawn for various shapes (cylindrical, brick, and platelet). Several plots illustrate the velocity, temperature, shear stress and heat transfer rate. Viscosity and thermal conductivity are evidently observed to be the most important physical quantities responsible for varying velocity and temperature profiles.

1. INTRODUCTION

From the previous few decades, nanofluids have been a major topic of importance among researchers. Nanofluid is an innovative way to improve the characteristics of heat transfer in liquids. It is particularly attractive because of its various industrial, biomedical, electronics, and transportation applications including hybrid engines, advanced nuclear systems, automobiles, biological sensors, drug delivery systems, etc. The average size of nanoparticles used in nanofluids may vary from 1 to 100 nm. Nanoparticles remain suspended almost indefinitely in fluids, reducing erosion and clogging dramatically compared to larger particles in suspension. In MHD (magnetohydrodynamic) nanofluid flow, the presence of magnetic fields can affect the heat transfer properties of the nanofluid. The interaction between the magnetic field and the nanoparticles can cause the particles to form chains or clusters, which can alter the flow behaviour and heat transfer characteristics of the nanofluid. Modeling, preparing, convective heat transfers, and characterization of nanofluids have been studied extensively. Aluminum is the most significant substance in technology. There are wide varieties of crystallographic variations with different properties of these substances. Corundum is the most frequently occurring form which is thermodynamically stable at room temperature. Many metastable polymorphs contain Al_2O_3.because Al_2O_3 has high thermal conductivity. Al_2O_3 nanoparticles are used to improve the heat transfer effect of thermal conductivity. Adding up to 1% Al_2O_3 increases the thermal conductivity of EG to 75%. The efficiency of a nanoparticle is not only influenced by the types of nanoparticles but also the shapes. Al_2O_3 typically spherical shaped nanoparticles, are used by researchers. However spherical-shaped nanoparticles have a restricted range of uses and relevance when compared. This is the reason when non-spherical nanoparticles like brick and platelet have been used in this investigation. The cylinder, platelet, and brick forms of nanoparticles are specifically included in this study. Moreover, square-shaped nanoparticles have a number of essential desired features that make them the major focus of present research, particularly in cancer therapy, according to the literature survey on nanofluids. Choi and Eastman [1] in this valuable research analysed, when nanoparticles are added to regular base fluids, their thermal conductivity and convection heat transfer rate increase significantly; these compositions are referred to as nanofluids. Nanofluids are base fluids suspension of nanoscale particles. Typically, various types of nanoparticles, which include metal, carbides, and oxides, and commonly used base fluids are EG, kerosene and propylene glycol. Aizar et al. [2] investigated the effect of thermal radiative and rate of heat transfer in mixed convection MHD flow of various-shaped nanoparticles of alumina in EG and water-based nanofluid. It was observed that cylindrical and platelet-shaped nanoparticles have lesser velocity than the blade and brick-shaped nanoparticles. This is related to the shear thinning characteristic of cylindrical-shaped nanoparticles in fluid, which causes temperature dependence in viscosity. Timofeeva et al. [3] looked into the effect of Al_2O_3 nanofluids including various shaped nanoparticles, this investigation contains both experimental and theoretical views. More specifically, the authors looked at various alumina-shaped nanoparticles in an EG and water-based fluid mixture of equal quantities. Hamilton and Crosser model has been used and observed that the thermal conductivity is enhanced due to

particle shape spherical nanoparticles were taken into account by Loganathan et al. [4] as the effects of thermal radiation on erratic convection flow of microfluids past an infinite vertical plate were investigated. It is observed that spherical-shaped Ag nanofluids are less kinetically active compared with Cu, TiO_2, and alumina nanofluids. Hatami and Ganji [5] and Hatami et al. [6] investigated the natural convection of $C_6H_9NaO_7$ non-Newtonian nanofluid flow between vertical plates. The GM and LSM have been developed and used in the problem of nanofluid flow and rate of heat transfer between two parallel plates caused by the normal motion of the porous upper plate respectively. Prasad et al. [7] theoretically analysed the heat transfer and MHD flow in a nanofluid over a slender elastic sheet with variable thickness. Ganesh et al. [8] numerically analyses the magnetic field affects the flow of water and ethylene glycol-based Al_2O_3 nanofluids across a flat surface in a Marangoni boundary layer. Sheikholeslami et al. [9] analysed the magnetohydrodynamic nanofluid flow and heat transfer of two horizontal parallel plates. Ilyas Khan and it has been shown by Khan and Khan [10] that viscous dissipation plays a critical role in the MHD Darcy flow in the presence of Cu-Np and that incompressible water-Cu and EG-Cu Newtonian nanofluids transport heat over a flat plate in the presence of Cu-Np. Water-copper nanofluids and EG-copper nanofluids exhibit the same increasing effect of nanoparticle volume fraction. Some relevant studies on the topic can be seen from the studies [11-18].

Since porous media is more permissible than non-porous media, the research on fluid flow and heat transfer in porous media is studied in the current literature. Heat transfer is directly proportional to the Hartmann number but inversely proportional to the Rayleigh number. Makinde and Mhone [19] who carried out an investigation of the unsteady flow field of a thin fluid through a channel filled with a porous medium when there is a combined effect of a transverse magnetic field and a radiative heat transfer. The results demonstrate that increase in magnetic field decreases the quality of wall shear stress while increasing the radiation parameter through heat absorption increases the amount of wall shear stress. Abbas et al. [20] analysed the oscillatory slip flow of electrically conducting viscous nanofluids through saturated porous media which are exposed to thermal radiation. In this work, it is observed that enhancement in SWCNTs and MWCNTs volume fractions increases the heat transfer rate at the boundaries and declines the temperature at the center of the channel. Waqas et al. [21] did a comparative study and analysed the numerical outcomes of hybrid nanofluid flow with heat radiation effect with cu, aluminum oxide, graphene oxide and ethylene nanoparticles over a stretching sheet. According to the study, the velocity profile increases with an increase in Deborah's number, whereas it decreases with an increase in magnetic parameter estimations. Das et al. [22] analysed the problem of free convection fluid flow through a vertical porous plate with heat and mass transfer through a porous media, the time-dependent permeability of a viscous flow incompressible electrically conducting fluid, whereas after a few years, Mishra et al. [23] modified the type of fluid to viscoelastic and analysed and it is noted that boundary layer flow is reduced by the heavier species with low conductivity. One can find more remarkable examples of the rate of heat transfer flow in studies [24-28] and the references therein.

Furthermore, reviews of the literature show that the majority of the previous studies in fluid flow are based on constant physical values, an although in a few cases, researchers investigate varying physical properties. Due to the significant influence of magnetic fields on channel flow, researchers have focused on MHD flow with heat and mass transfer in permeable media. This has numerous applications, which include MHD power generators, nuclear reactor cooling, plasma studies and geothermal energy extraction. Additionally, the study of oscillatory flow is crucial for solving many engineering and physiological issues, like blood flow through arteries, water pumps and fuel pumps, in view of these applications. Narayana et al. [29], the knowledge from the current study will be helpful for many industrial applications (which are like cooling of electronic devices) and scientific, where it is essential to avoid disturbance in the assembly chips by oscillations. It is noted that the oscillatory flow enhances the heat transfer rate. The heat is transported axially because the fluid oscillates at high frequency with large total displacement, so larger quantities of heat are transported. Srinivasacharya and Mendu [30] have taken into account how the first-order chemical reaction, radiation and magnetic field effects affect the free convection heat and mass transfer over a vertical plate with irregular wall conditions for temperature and concentration and it is found that increasing radiation parameter leads to an increase in Nusselt number, Sherwood number, skin friction coefficient and a fall in wall couple stress. A homogeneous chemical reaction of magneto micropolar fluids, which pass through vertical plates with slip flow, is examined by Chaudhary and Jha [31]. The author concludes that translational velocity increases with increasing values of the permeability parameter, but the microrotation profile tends to decrease with an increase in various values of permeability. Hamilton and Crosser [32] both theoretically and experimentally analysed the thermal conductivities of various types of two components mixture in which heterogeneous were correlated. The author concluded by giving an equation that determines the empirical shape factor based on the thermal conductivities of the phases and the shape of the particles can be used to calculate thermal conductivities for heterogeneous two-component systems. Jafar et al. [33] consider the combined effect of various parameters on the MHD flow of nanofluid through a nonlinear stretching sheet in porous media. The study reveals that the raise in the volume fraction parameters enhance the velocity and temperature. Shoaib et al. [34] analysed a significant amount of research that has been conducted on the production, classification, and uses of various types of Nps. However, hybrid nanofluids are of more recent type that is produced using two or more types of nanoparticles, either in mixed or compound form. The main goal of this technique is to make the ideal simultaneous combination of several materials' chemical and physical characteristics in a special building. Authors have also paid close attention related to this investigation [35-37].

Sedki [38] examines the influence of internal heat with permeable stretching/shrinking wedges variable k_{nf} and μ_{nf} on unsteady MHD induces in convective boundary wall flow of various incomprehensible electron conducting fluid in the presence of internal heat. The author observed that as the surface nonlinearity, Brownian motion, chemical reaction and permeability raises, the heat transfer rate increases but the reverse occurs with the volume fraction.

Kataria and Patel [39] analysed the radiation, chemical reaction, Soret and heat generation effects on MHD Casson nanofluid in oscillating vertical channel through porous media. It is noticed that with an increase in Casson parameter, the velocity decreases, this is due to the viscous force in the fluid

which drags the fluids whereas Patel [40] investigated a similar kind of study without chemical reaction parameters and concluded that the concentration of the fluid is enhanced when the chemical reaction parameter is raised. Sasikumar et al. [41] analysed the rate of heat transfer, mass transfer and chemical reaction effect with slip in the asymmetric channel. It is noted that the heat transfer rate rises in both the channel walls with varying values of time. Sasikumar et al. [42] studied the impact of heat and mass transfer rate on MHD oscillatory flow in an asymmetric tapered channel. The study investigates various parameters that influence the flow and heat transfer characteristics. It is observed that as the Peclet number rises, the temperature tends to decrease, while the temperature tends to increase with higher radiation parameters.

The effects of chemical reactions and viscous dissipation on MHD free convection flow are studied analytically by Pal and Biswas [43] in the presence of heat sources and sinks, thermal radiation, and variable surface temperatures and concentrations and it is observed that enhancement in magnetic field parameter decreases the skin friction coefficient. Gupta et al. [44] analyses a model of the 3-D flow of Cu-water and alumina water Nf over an exponentially stretching sheet. Cu-water and Al_2O_3-water simultaneous effects for convective conditions of magnetic field radiation over 3-D flow. It is found that the alumina water nanofluid has a thicker momentum boundary layer when compared with copper-water nanofluid. Zeeshan et al. [45] investigate the non-Newtonian couple stress fluid over the upper horizontal surface of the parabola of the reacting catalytic surface of the double-diffusive stretching fluid and the velocity and temperature profile are generated graphically for various parameters. Modather et al. [46] investigated the impact of a chemical reaction on the heat and mass transfer of micropolar fluids over an infinitely moving permeable plate in a saturated porous medium. It has been analysed that the chemical reaction parameter or permeability parameter when increased the velocity also increases whereas the temperature falls. References [47-51] provide a list of some recent researchers who have studied the MHD oscillatory flow in various fields.

It is evident from the above literature survey that how the addition of nanoparticles to the base fluid can significantly increase its thermal conductivity and convective heat transfer coefficient, resulting in more efficient heat transfer. Overall, these studies demonstrate the importance of considering the size and shape of nanoparticles in MHD nanofluid flow and heat transfer analysis. The results suggest that the choice of nanoparticle size and shape can significantly affect the flow behaviour, heat transfer characteristics, and pressure drop of the nanofluid, which has important implications for the design and optimization of MHD nanofluid-based heat transfer systems.

From the above literature survey, we observe that there is no problem analysis on MHD nanofluid combined with oscillatory flow types, thermal radiation effect and specific geometries like asymmetric wavy and tapered wavy channels. It is evident that there is no report on heat transfer characteristic of oscillatory nanofluid flow of various shapes and different types of nanoparticles. This creates scope for new research and motivated the present work analysing the effect of various shapes and types of nanoparticles on heat transfer characteristics of oscillatory magnetic nanofluid flow through asymmetric wavy channel in the presence of thermal radiation.

As a result, the goal of the present study is planned to design and solve the research issues listed below:

- What is the influence of copper (Cu), gold (Au), silver (Ag), and alumina (Al_2O_3) nanoparticles on the velocity field, temperature field and heat transfer regime?
- How do the shear stress and heat transfer rate change with the rising thermal radiation parameter?
- What is the significance of various shapes of nanoparticles on the velocity field?

The remaining part of the paper is organized into various sections as follows: In Section 2, the mathematical model for the fluid flow problem is formulated in the form of governing equations with a set of boundary conditions. The non-dimensional quantities are defined by non-similarity transformation through which the governing equations and boundary conditions are obtained in non-dimensional form. Section 3, includes a solution procedure for solving the governing equations subject to boundary conditions. The exact solutions of the velocity profile, temperature profiles, skin friction coefficient and Nusselt number are obtained. In Section 4, the graphs are generated using MATLAB software for the velocity field, temperature field, skin friction coefficient and heat transfer rate. The discussion on the results obtained by analysing graphs and tables of various flow profiles is presented. Conclusions with limitations and scope for future research work are drafted in Section 5.

2. MATHEMATICAL FORMULATION OF THE PROBLEM

It has been proposed that optically thin viscous fluid in asymmetric wavy channel that are incompressible and electrically conducting is considered.

$$H_1 = d_1 + a_1 \cos\frac{2\pi x}{\lambda}$$
$$H_2 = -d_2 - b_1 cos\frac{2\pi x}{\lambda} + \varphi \quad (1)$$

where, a_1, b_1, d_1, d_2 and φ which satisfies the condition $a_1^2+b_1^2+2a_1b_1\cos\varphi\leq(d_1+d_2)^2$ [29]. The oscillation is the phase difference (φ) which is between the range of $0\leq\varphi\leq\pi$. where, φ=0 corresponds the symmetrical channel with waves out of phase φ=π in Figure 1. The temperature on the boundaries is kept at T_1 and T_2, which is high enough to promote radiative heat transfer. The induced magnetic field is believed to be insignificant since the Reynolds number and transversely applied magnetic field are both very small. The oscillating pressure-gradient (λ) across channel ends and irregular walls cause the fluid to oscillate. The viscous and Darcy's resistance of the elements is addressed properly with constant k_1.

According to Boussinesq's approximation, momentum and energy can be expressed using the following equations [29]:

$$\rho_{nf}\frac{\partial u}{\partial t} = -\frac{\partial p}{\partial x} + \mu_{nf}\frac{\partial^2 u}{\partial y^2} - \left(\sigma B_0^2 + \frac{\mu_{nf}}{k_1}\right)u + g(T - T_0) \quad (2)$$

$$\left(\rho c_p\right)_{nf}\frac{\partial T}{\partial t} = k_{nf}\frac{\partial^2 T}{\partial y^2} - \frac{\partial q}{\partial y} \quad (3)$$

The below equations are boundary conditions:

$$u = 0, T = T_1 \; on \; y = H_1$$
$$u = 0, T = T_2 \; on \; y = H_2 \tag{4}$$

The fluid velocity across x-axis is represented by u=u (y, t) and the temperature are represented by T=T (y, t), the density of Nf is ρ_{nf}, μ_{nf} is the dynamic viscosity of Nf, $k_1>0$ is the permeability of the porous media, ' σ ' is the electrical conductivity of the base fluid, 'g' is the acceleration due to gravity, k_{nf} is the thermal conductivity of Nf, radiative heat flux in x-axis is represented by q and $(\rho\beta)_{nf}$ and $\left(\rho c_p\right)_{nf}$ are the thermal expansion coefficient and heat capacitance of nanofluids respectively.

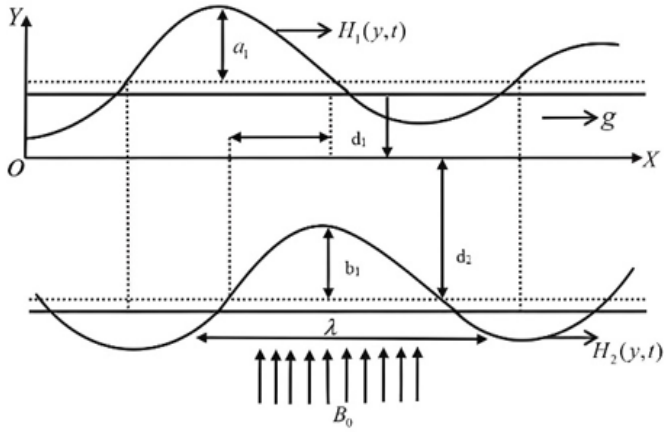

Figure 1. Physical configuration of problem

In order to analyse spherical and non-spherical shaped nanoparticles the conductivity k_{nf} and dynamic viscosity μ_{nf} are chosen based on Hamilton and crosser model [32].

$$\mu_{nf} = \mu_f(1 + a\phi + b\phi^2) \tag{5}$$

$$\frac{k_{nf}}{k_f} = \frac{k_s + (n-1)k_f + (n-1)\left(k_s - k_f\right)\phi}{k_s + (n-1)k_f - \left(k_{s-}k_f\right)\phi} \tag{6}$$

$$\begin{gathered}\rho_{nf} = (1-\phi)\rho_f + \phi\rho_s \\ (\rho\beta)_{nf} = (1-\phi)(\rho\beta)_f + \phi(\rho\beta)_s \\ \left(\rho c_p\right)_{nf} = (1-\phi)\left(\rho c_p\right)_f + \phi\left(\rho c_p\right)_s\end{gathered} \tag{7}$$

The empirical shape factor n is determined as 3/ψ, where ψ is represented as the ratio between the region of the actual particle to the region of a sphere with equal masses.

In the work of Makinde and Mhone [19], the plate temperature T_o and T_w are usually high and produces radiative heat transfer. According to Cogley et al. [11] for optically thin medium with relatively low density the radiative heat flux is given by:

$$\frac{\partial q}{\partial y} = -4\alpha^2(T - T_0) \tag{8}$$

Eq. (8) is Substituted in Eq. (3).

$$\left(\rho c_p\right)_{n\rho f}\frac{\partial T}{\partial t} = k_{nf}\frac{\partial^2 T}{\partial y^2} + 4\alpha^2(T - T_0) \tag{9}$$

where, α is the radiation absorption coefficient.

Introducing the following dimensionless variables:

$$\begin{gathered}x^* = \frac{x}{d},\ y^* = \frac{y}{d},\ u^* = \frac{u}{U_0},\ t^* = \frac{tU_0}{d},\ p^* = \frac{d}{\mu U_0}p,\ b = \frac{b_1}{d_1} \\ T^* = \frac{T-T_0}{T_w-T_0},\ \omega^* = \frac{d\omega}{U_0},\ \lambda_n = \frac{k_{nf}}{k_f}, Re = \frac{U_0 d}{v_f},\ M^2 = \frac{\sigma B_0^2 d^2}{\mu_f}, \\ K = \frac{k_1}{d^2},\ Gr = \frac{g\beta_f d^2(T_w-T_0)}{v_f U_0},\ Pe = \frac{U_0 d\left(\rho c_p\right)_f}{k_f},\ N^2 = \frac{4d^2\alpha^2}{k_f}, \\ d = \frac{d_2}{d_1},\ a = \frac{a_1}{d_1}\end{gathered} \tag{10}$$

The boundary conditions in non-dimensional form become:

$$h_1 = 1 + a\,cos(2\pi x) \text{ and } h_2 = -d - b\,cos(2\pi x + \varphi)$$

As a, b, d and φ satisfy the condition:

$$a^2 + b^2 + 2ab\,cos\,\varphi \le (1+d)^2$$

Using Eq. (5), Eq. (6) in Eq. (2), Eq. (9), (omitting* symbol)

$$\begin{gathered}(\phi_1)Re\frac{\partial u}{\partial t} = \lambda e^{i\omega t} + (\phi_2)\frac{\partial^2 u}{\partial y^2} - M^2 u - \frac{\phi_2}{K}u \\ + (\phi_3)Gr\theta\end{gathered} \tag{11}$$

$$Pe\frac{\phi_4}{\lambda_n}\frac{\partial\theta}{\partial t} = \frac{\partial^2\theta}{\partial y^2} + \frac{N^2}{\lambda_n}\theta \tag{12}$$

where, $\phi_1, \phi_2, \phi_3\ and\ \phi_4$ are the constants used to simplify Eq. (2), Eq. (9) into Eq. (11), Eq. (12).

$$\phi_1 = (1-\phi) + \phi\frac{\rho_s}{\rho_f},\ \phi_2 = (1 + a\phi + b\phi^2),$$
$$\phi_3 = (1-\phi)\rho_f + \phi\frac{(\rho\beta)_s}{\beta_f},\ \phi_4 = \left[(1-\phi) + \phi\frac{(\rho c_p)_s}{(\rho c_p)_f}\right]$$

Further, the above constants are substituted in Eq. (11), Eq. (12) and grouped as below constants.

$$a_0 = \varphi_1 Re,\ m_0^2 = M^2 + \frac{\varphi_2}{k},\ a_3 = \varphi_3 Gr,\ b_0^2 = \frac{Pe\varphi_4}{\lambda_n},\ b_3^2 = \frac{N^2}{\lambda_n}$$

After simplifying (11) and (12), take the forms:

$$a_0\frac{\partial u}{\partial t} = \frac{\partial p}{\partial x} + \phi_2\frac{\partial^2 u}{\partial y^2} - m_0^2 u + a_3\theta \tag{13}$$

$$b_0^2\frac{\partial\theta}{\partial t} = \frac{\partial^2\theta}{\partial y^2} + b_3^2\theta \tag{14}$$

In non-dimensional form, the associated boundary conditions are as follows:

$$u = 0, \theta = 1\ on\ y = h_1, u = 0, \theta = 0\ on\ y = h_2 \tag{15}$$

3. METHOD OF SOLUTION

The partial differential Eq. (13), Eq. (14) converted to ordinary differential equation by taking the pressure gradient purely oscillatory, velocity and temperature for oscillatory flow as (see Refs. [23, 26, 41, 47]):

$$\begin{gathered}\mathrm{u(y,t)} = \mathrm{u_0(y)e^{i\omega t}} \\ \theta(y,t) = \theta_0(y)e^{i\omega t}\end{gathered} \tag{16}$$

$$-\frac{\partial p}{\partial x} = \lambda e^{i\omega t}$$

3.1 Calculation

On substituting (16) on (13) and (14), we obtain the below the ordinary differential equations,

$$\frac{d^2u_0}{dy^2} - m_1^2 u_0 = \frac{-\lambda}{\phi_2} - \frac{a_3\theta_0}{\phi_2} \tag{17}$$

$$\frac{d^2\theta_0}{dy^2} + m_2^2\theta_0 = 0 \tag{18}$$

where, $m_1^2 = \frac{m_0^2 - a_0 i\omega}{\phi_2}$, $m_2^2 = b_3^2 - b_0 i\omega$

The below equations are the boundary conditions:

$$\begin{aligned} u_0 = 0, \theta_0 = 1 \; on \; y = h_1 \\ u_0 = 0, \theta_0 = 0 \; on \; y = h_2 \end{aligned} \tag{19}$$

The solution is obtained for $u(y,t)$ (velocity) and $\theta(y,t)$(temperature) by solving Eq. (17), Eq. (18) under the boundary conditions (19).

$$\begin{aligned} &u(y,t) \\ &= \left(1 - e^{m1(y-h_2)}\right)\frac{\lambda}{\phi_2 m_1}e^{i\omega t} \\ &+ \frac{a_1}{\phi_2(m_2 - m_1)}\frac{\sin m_2(y-h_2)}{\sin m_2(h_1-h_2)}e^{i\omega t} \\ &- \left[\frac{\lambda}{\phi_2 m_1} + \frac{a_1}{\phi_2(m_2-m_1)}\right. \\ &\left. - \frac{\lambda}{\phi_2 m_1}e^{m_1(h_1-h_2)}\right]\left[\frac{\sinh m_1(y-h_2)}{\sinh m_1(h_1-h_2)}\right]e^{i\omega t} \end{aligned} \tag{20}$$

$$\theta(y,t) = \frac{sin\, m_2(y-h_2)}{sin\, m_2(h_1-h_2)}e^{i\omega t} \tag{21}$$

The Shear Stress (τ) along the walls of the channel is given by:

$$\begin{aligned} \tau &= \mu\left\{\frac{\partial u}{\partial y}\right\}_{y=h_1,h_2} \\ &= \mu\left\{\left(-e^{m1(y-h_2)}\right)\frac{\lambda}{\phi_2}e^{i\omega t}\right\} \\ &+ \mu\left\{\frac{a_1}{\phi_2(m_2-m_1)}\right\}\frac{m_2\cos m_2(y-h_2)}{\sin m_2(h_1-h_2)}e^{i\omega t} \\ &- \mu\left\{\left[\frac{\lambda}{\phi_2 m_1} + \frac{a_1}{\phi_2(m_2-m_1)}\right.\right. \\ &\left.\left. - \frac{\lambda}{\phi_2 m_1}e^{m_1(h_1-h_2)}\right]\left[\frac{m_1\cosh m_1(y-h_2)}{\sinh m_1(h_1-h_2)}\right]\right\}e^{i\omega t} \end{aligned} \tag{22}$$

The rate of heat transfer along the walls of the channel is given by:

$$Nu = -\left(\frac{\partial\theta}{\partial y}\right)_{y=h_1,h_2} = \frac{-m_2\cos m_2(y-h_2)}{\sin m_2(h_1-h_2)}e^{i\omega t} \tag{23}$$

4. RESULTS AND DISCUSSION

The heat transfer characteristics of MHD oscillatory Nf flow inside the wavy channel filled with porous media are studied. Ethylene glycol (EG) ($C_2H_6O_2$) and water (H_2O) as the base fluid, four different kinds of nanoparticles are considered: copper (Cu), gold (Au), silver (Ag), and alumina (Al_2O_3) from Table 1. Three various shapes such as cylinder, platelet, and brick are examined for nanoparticles using Table 2. The analytic method is being used to solve the governing partial differential equations with boundary conditions.

Table 1. Thermophysical properties of base fluids and nanoparticles [4, 12, 13].

Model	ρ (kgm^{-3})	c_p $(kg^{-1}K^{-1})$	K $(Wm^{-1}k^{-1})$	βX10^{-5} (K^{-1})
H_2O	997.1	4179	0.613	21
$C_2H_6O_2$	1115	0.58	0.1490	6.5
Al_2O_3	3970	765	40	0.85
Ag	10500	235	429	1.89
Cu	8933	385	401	1.67
Au	19300	129	318	2.2

Table 2. Sphericity ψ and constants a and b for different shapes of nanoparticles [3]

Model	Platelet	Brick	Cylinder
a	37.1	1.9	13.5
b	612.6	471.4	904.4
Ψ	0.52	0.81	0.62

In Figure 2 the influence of varying shapes of nanoparticle of Al_2O_3-water based nanofluid in velocity distribution is examined. It is observed that platelet shaped nanoparticle has lower velocity followed by cylinder shaped and brick shaped nanoparticle. Since k_{nf} and μ_{nf} are higher, platelet shaped alumina-water based nanofluid's magnitude of velocity is minumum compared to cylinder and brick shaped nanoparticles.

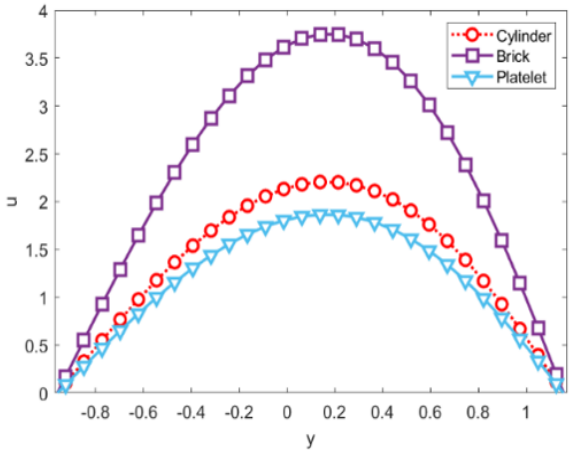

Figure 2. Velocity profile of varying shapes of Al_2O_3-H_2O $\lambda = 1, t = 10, \omega = \frac{\pi}{4}, K = 1, \varphi = 0.04$

It is observed in Figure 3 that brick shaped Al_2O_3 nanoparticle has higher velocity when compared with platelet and cylinder-shaped nanoparticle. For ϕ<0.1, the shapes have strong influence on the velocity of nanofluid due to the strong dependence of viscosity on particle shape. According to the present study, cylinder and platelet shaped nanoparticle have the higher viscosity compared to brick shaped nanoparticle.

The acquired results are in line with the experimental results of Timofeeva et al. [3] which reports that the platelet shaped nanoparticle has higher viscosity when compared with spherical shaped nanoparticle also they examined their outcomes to those of Hamilton and Crosser [32] and discovered that the two model findings are same.

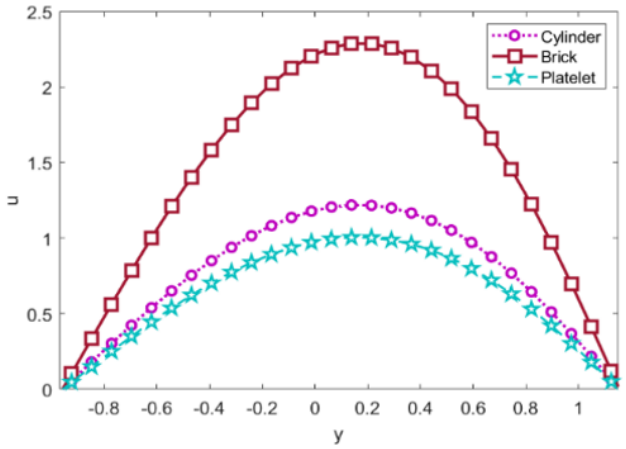

Figure 3. Velocity profile of varying shapes of Al_2O_3-EG Nf $\lambda = 1, t = 0.1, \omega = \frac{\pi}{4}, K = 1, \varphi = 0.04$

Table 3. Authentication of the results of θ for various values of φ when t=0.1, *Pe*=0.71, N=0.1

φ	Ref. [2]	Present Analysis
0.04	1.0017	1.0018
0.03	1.0016	1.0017
0.02	1.0015	1.0016
0.01	1.0014	1.0015

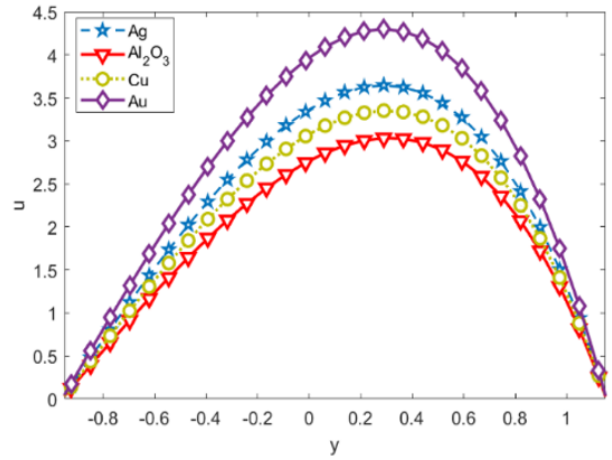

Figure 4. Velocity comparison due to various Np in H_2O-Nfs $\lambda = 1,\ t = 10, \omega = \frac{\pi}{4}, M = 1, K = 1, \varphi = 0.04$

The influence of different nanoparticles of platelet shape is analysed in Figure 4. It is found that the velocity of water-based Nf is higher for Au nanoparticles followed by Ag, Cu and Al_2O_3 nanoparticle. It can also be interpreted as Al_2O_3 water-Nf has higher μ_{nf} and k_{nf} followed by Cu, Ag and Au. This result is also supported by Hamilton and Crosser [32]. A comparison of Al_2O_3-water and Al_2O_3-EG based nanofluid in platelet shape is made in Figure 5. It is observed that EG based Nf has higher viscosity than water-based Nf. As water based nanofluid has higher velocity than EG based Nf for some values of volume fraction. Hamilton and Crosser [32] have also predicted the k_{nf} and μ_{nf} of water and EG based Nf. The current findings are related to the available works [2], as shown in Table 3. The rate of heat transfer in Aaiza et al. [2] is calculated and compared with the present study by considering $a_1 = 0, a_2 = 0, b_1 = 0, b_2 = 0$ and compared with the present study to validate the problem.

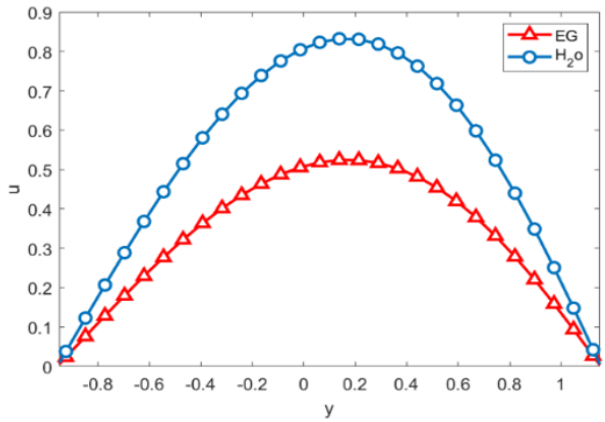

Figure 5. Velocity comparison graph of EG and water based nanofluid when $\lambda = 1, t = 10, \omega = \frac{\pi}{4}, Pe = 0.71, M = 1, N = 0.1, K = 1, \varphi = 0.04$

The effect of axial velocity for varying values of magnetic field parameter (M) in brick shaped Au-EG nanofluid is observed in Figure 6. When the magnetic field parameter increases the velocity decreases. This is because, when the magnetic field M on an electrically conducting fluid is increased, a resistive Lorentz force is produced, that is comparable to drag force. The drag force falls as the magnetic field rises, by slowing down the fluid velocity. According to Hamilton and Crosser [32], for different values of ϕ of platelet shaped copper-EG-Nf, the velocity decreases with increase in the different values of ϕ in Figure 7. Cogley et al. [11] their experiment has also reported the same. The influence of velocity for different values of Grashof number of platelet shaped alumina-EG nanofluid is shown in Figure 8. It is observed that the increase in Grashof number, increases the velocity. The rise in Gr that is Grashof number, increases the temperature gradient which leads to increase in buoyancy force. Therefore, the velocity increases. The velocity profile for different values of permeability parameter i.e., k of cylindrical shaped alumina water nanofluid is analysed in Figure 9. It is found that when k increases the velocity also increases. This is due to Darcy's law. The effect of temperature with different values of thermal radiation of cylindrical shaped Au-water Nf is analysed in Figure 10. The increase in thermal radiation, increases the temperature, which means the effect of energy transfer to the fluid is most. The effect of oscillatory parameter in brick shaped alumina water nanofluid is analysed in Figure 11. It is noted that when the oscillatory parameter ω increases, the temperature profile decreases.

In Figure 12, the influence of different nanoparticles in the temperature profile for cylindrical shape in water-based nanofluid is observed. It is noted that cylindrical-shaped Al_2O_3 nanoparticle has higher temperature followed by copper, silver and gold in water based Nf. The cylindrical shaped Al_2O_3 - water and Al_2O_3-EG based nanofluid on temperature profile is compared on Figure 13. The viscosity of EG-based Nf is found

to be greater than water-based nanofluid. For various values of volume fraction, water-based Nf has a higher temperature than EG-based nanofluid. The effect of temperature with different values of thermal radiation of cylindrical shaped Au-water nanofluid is observed in Figure 14. The rise in N increases the temperature, which means the effect of energy transfer to the fluid is most.

The effect of oscillatory parameter in brick shaped alumina water nanofluid is analysed in Figure 15. It is noted that when the oscillatory parameter ω rises, the temperature profile falls. The influence of different values of ϕ on cylindrical shaped copper nanoparticle in EG nanofluid on temperature is analysed in Figure 16. It is noted that the rise in volume fraction, decreases the temperature. This was practically studied and shown by Timofeeva et al. [3]. The effect of varying values of Pe number in temperature for platelet shaped Ag water nanofluid is analysed in Figure 17. It is observed, when Pe increases the temperature decreases. The effect of Shear Stress on platelet shaped Al_2O_3-water nanoparticle for different values of Grashof number over the boundaries are made in Figure 18. It is observed that τ vary periodically due to asymmetric surface motion. Figure 19 displays the Shear Stress for various values of N on platelet shaped Cu-water nanofluid.it is seen that the τ falls at the channel wall $y=h_1$ (left wall) and increases at the channel wall $y=h_2$ (right wall) with increase of thermal radiation.

Figure 20 displays the heat transfer coefficient for various values of N on platelet shaped Al_2O_3-EG nanofluid. It is seen that the heat transfer rate falls at the channel wall $y=h_1$ (left wall) and rises at the channel wall $y=h_2$ (right wall) with increase in thermal radiation. Table 4, represents the heat transfer rate for various values of volume fraction, Peclet number and thermal radiation. The rate of heat transfer for platelet shaped Cu-EG and Cu-water nanofluid over the channel wall $y=h_1$ is compared in Figure 21. It is observed that Cu-EG nanofluid has higher heat transfer rate when compared with Cu-water based nanofluid. In Figure 22 and Figure 23 the heat transfer for various nanoparticles of platelet shaped in water nanofluid over the two walls $y=h_1$ and $y=h_2$ are noted. It is observed that the rate of heat transfer increases for Al_2O_3 and followed by Cu, Ag and Au where as in the right wall h_2 it is reversed.

Table 4. Effect of dimensionless parameters on *Nu* for nanoparticles

φ	Pe	λ	N	Nusselt Number			
				Al_2O_3	Cu	Ag	Au
0.01	1.0	0.5	1.0	0.6604	0.6605	0.6604	0.6604
0.02				0.6603	0.6604	0.6602	0.6602
0.03				0.6602	0.6603	0.6601	0.6601
0.04				0.6601	0.6603	0.6599	0.6599
	1.5			0.6830	0.6830	0.6828	0.6829
	2.0			0.7138	0.7140	0.7136	0.7137
	2.5			0.7138	0.7526	0.7521	0.7521
	3.0			0.7980	0.7983	0.7976	0.7976
		0.5		0.3236	0.3238	0.3233	0.3233
		1.0		0.6604	0.6605	0.6604	0.6604
		1.5		0.7746	0.7746	0.7746	0.7746
		2.0		0.8314	0.8314	0.8314	0.8314
			1.0	0.6604	0.6605	0.6604	0.6604
			1.5	0.1347	0.1347	0.1346	0.1346
			2.0	-0.8551	-0.8550	-0.8553	-0.8553
			2.5	-3.1011	-3.1006	-3.1017	-3.1017

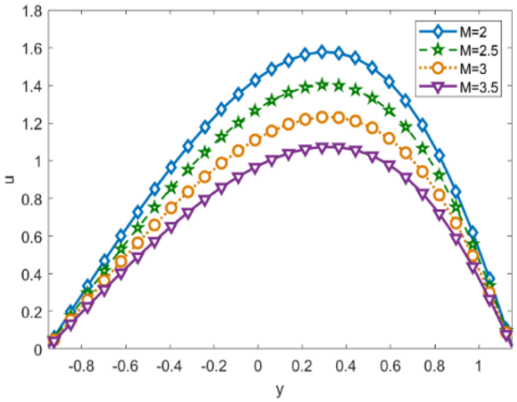

Figure 6. Effect of Hartmann number on velocity profile when $\lambda = 1, t = 10, \omega = \frac{\pi}{4}, K = 0.1, \varphi = 0.04$

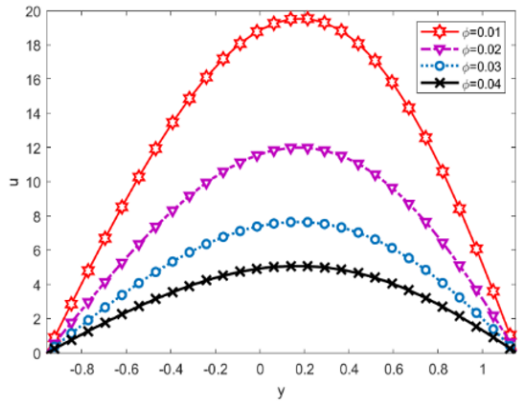

Figure 7. Effect of ϕ on velocity profile when $\lambda = 1, t = 10, \omega = \frac{\pi}{4}, K = 1, M = 1$

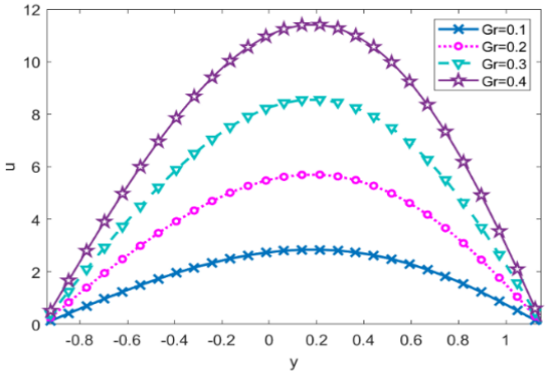

Figure 8. Effect of Grashof number on velocity profile when $\lambda = 1, t = 10, \omega = \frac{\pi}{4}, K = 1, \varphi = 0.04, M = 1$

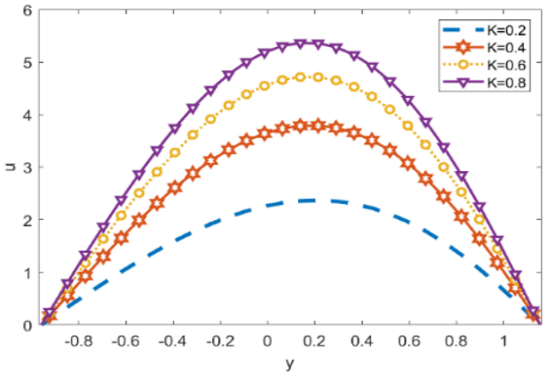

Figure 9. Effect of k on velocity profile when $\lambda = 1, Pe = 0.71, t = 10, \omega = \frac{\pi}{4}, N = 2, \varphi = 0.04$

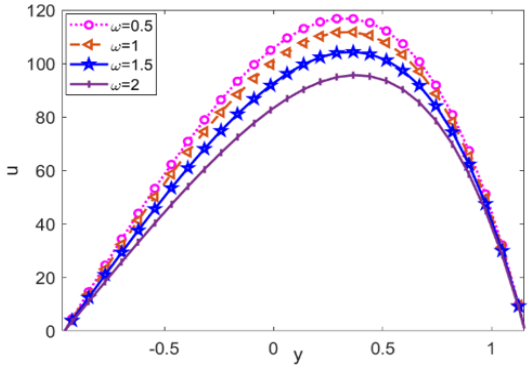

Figure 10. Effect of ω on velocity profile when $\lambda = 1, t = 0.1, Pe = 0.71, N = 0.5, K = 1, \varphi = 0.04$

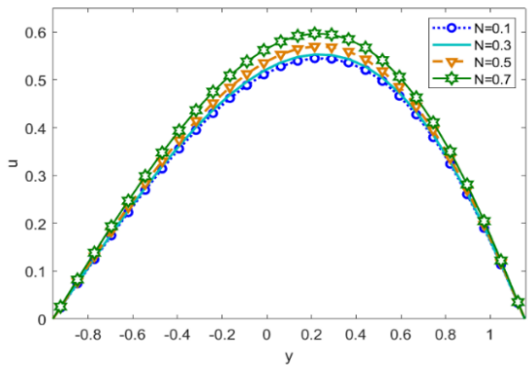

Figure 11. Effect of N on velocity profile when $\lambda = 1, t = 10, \omega = \frac{\pi}{4}, K = 1, \varphi = 0.04$

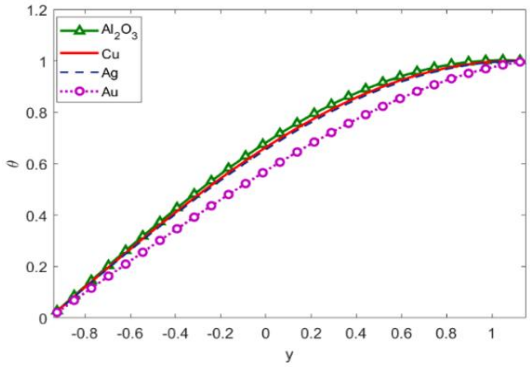

Figure 12. Temperature distribution due to various Np when $\lambda = 1, t = 0.1, \omega = \frac{\pi}{4}, Pe = 0.71, N = 1, K = 1, \varphi = 0.04$

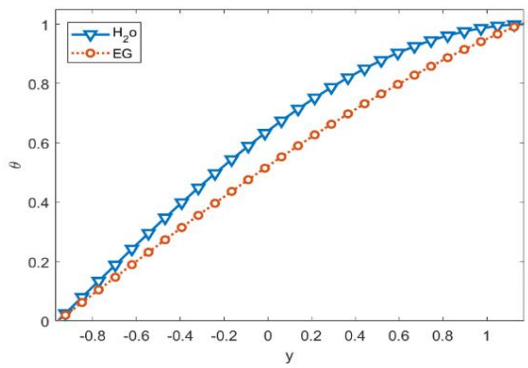

Figure 13. Temperature comparison of EG and H_2O based Nf when $\lambda = 1, t = 0.1, \omega = \frac{\pi}{4}, N = 2, K = 1, \varphi = 0.04$

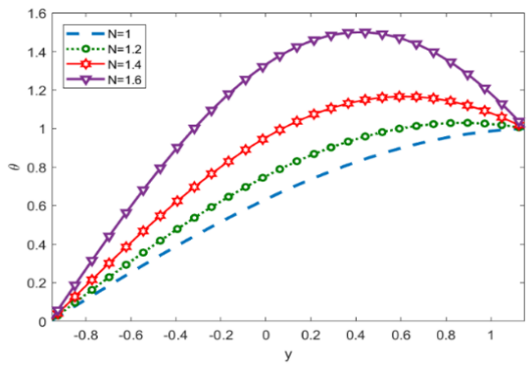

Figure 14. Effect of N on temperature profile when $\lambda = 1, t = 0.1, \omega = \frac{\pi}{4}, Pe = 1, K = 1, \varphi = 0.04$

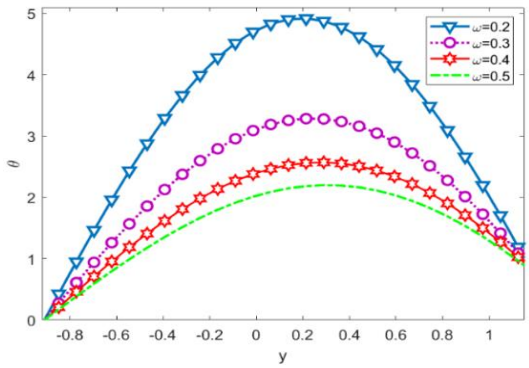

Figure 15. Effect of ω on temperature profile when $\lambda = 1, t = 0.1, Pe = 0.71, N = 2, K = 1, \varphi = 0.04$

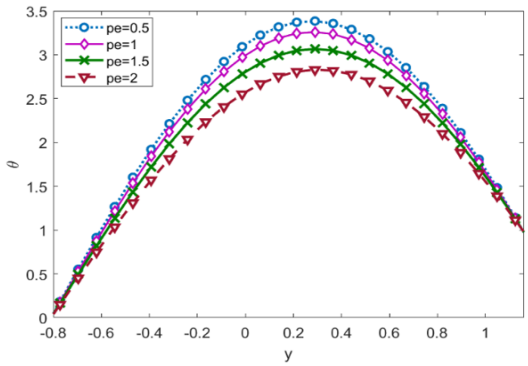

Figure 16. Effect of Pe on temperature profile when $\lambda = 1, t = 0.1, \omega = \frac{\pi}{4}, N = 2, K = 1$

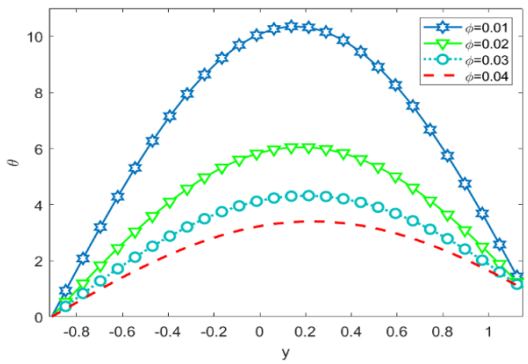

Figure 17. Effect of ϕ on temperature profile when $\lambda = 1, t = 0.1, \omega = \frac{\pi}{4}, N = 2, K = 1$

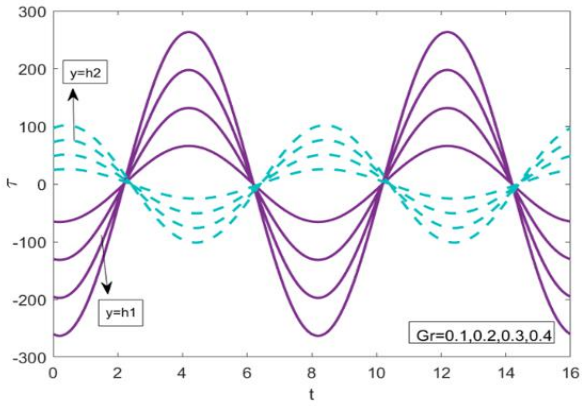

Figure 18. Shear stress for varying values of Gr when $\lambda = 1, \omega = \frac{\pi}{4}, Pe = 1, N = 2, K = 1$

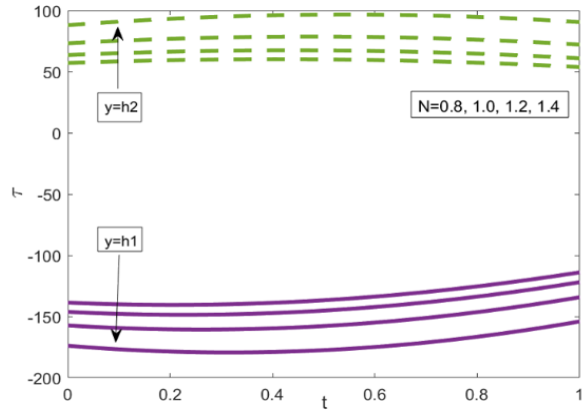

Figure 19. Shear Stress for varying values of N when $\lambda = 1, \omega = \frac{\pi}{4}, Pe = 1, Gr = 1, K = 1$

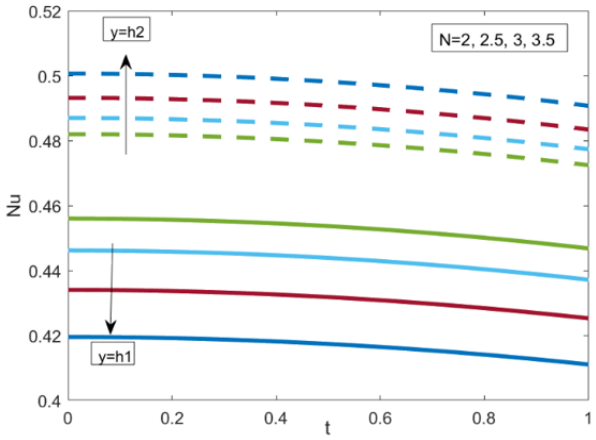

Figure 20. Heat transfer at the walls for varying values of N when $\lambda = 1, \omega = \frac{\pi}{4}, Pe = 1, N = 2, K = 1$

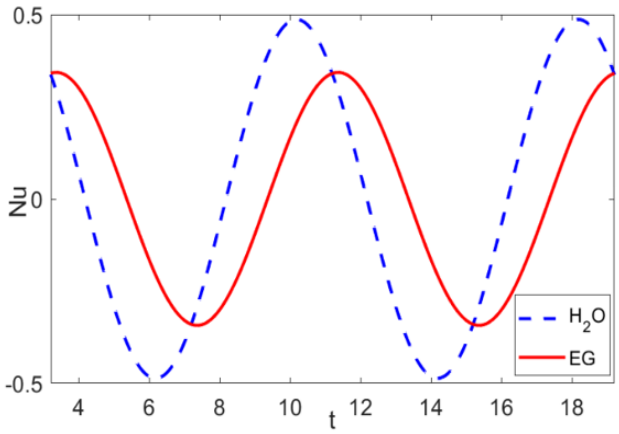

Figure 21. Heat transfer of comparison of base fluids at $y=h_1$ when $\lambda = 1, \omega = \frac{\pi}{4}, Pe = 1, N = 2, K = 1$

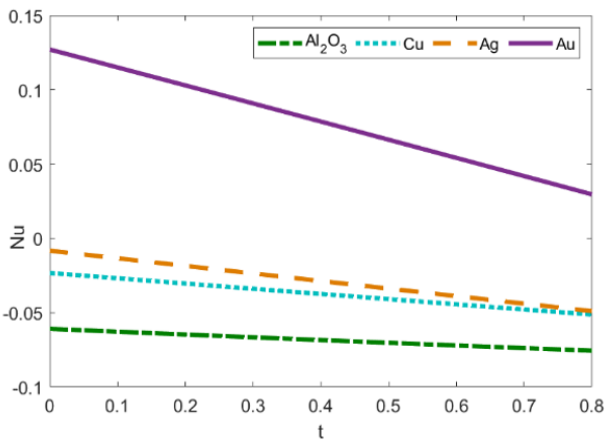

Figure 22. Heat transfer at the wall $y=h_2$ for varying nanoparticle in water-based nanofluid when $\lambda = 1, \omega = \frac{\pi}{4}, Pe = 1, N = 2, K = 1$

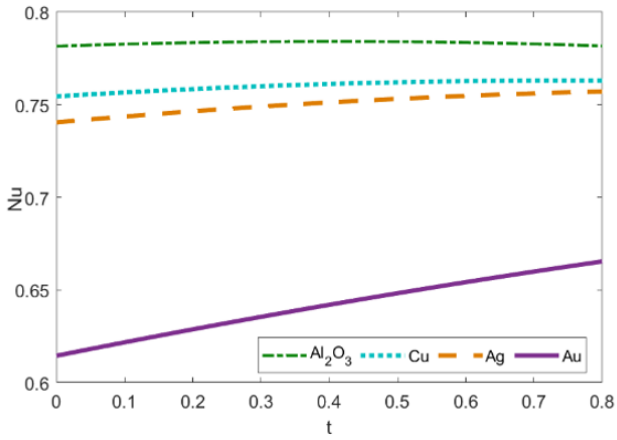

Figure 23. Heat transfer at the wall $y=h_1$ for varying nanoparticle in water-based nanofluid when $\lambda = 1, \omega = \frac{\pi}{4}, Pe = 1, N = 2, K = 1$

5. CONCLUSIONS

We have investigated the impact of heat transfer on MHD oscillatory nanofluid flow with thermal radiation for three various shapes and four different nanoparticles in this research. The nonlinear governing equations are solved by analytical method for velocity and temperature profiles.

The following are the major conclusions:

- The cylindrical shaped and platelet shaped nanoparticle have lesser velocity when compared to brick

shaped nanoparticle Al_2O_3-water nanofluids.

- It is noted that Au has higher velocity followed by Ag, Cu and Al_2O_3 of platelet shaped water based nanofluid.
- Velocity of Al_2O_3 nanofluid of cylindrical shape are compared for water and EG base fluid. It is observed that the Al_2O_3-water nanofluid has higher velocity when compared with Al_2O_3 -EG nanofluid.
- The fluid velocity decreases with increase in Hartmann number or volume fraction or oscillatory parameter whereas velocity increases with the increase in permeability parameter or Grashof number or thermal radiation.
- The fluid temperature increases with increase in thermal radiation and decreases with the increase in Peclet number or volume fraction.
- The Al_2O_3 water nanofluid has higher temperature profile followed by Cu, Ag and Au water based nanofluid of platelet shape.
- The heat transfer rate falls at the channel wall $y=h_1$ and increases at the other wall $y = h_2$ with the increase of thermal radiation.

In the current research, the effect of variable viscosity, entropy generation, chemical reaction etc. on the problem of MHD nanofluid flow is not taken into consideration. The future research for this study can be modelled for the above mentioned ignored quantities with hybrid or ternary nanofluids. Numerical schemes such as RK4, shooting technique, and finite difference schemes can be used to solve the governing equations.

ACKNOWLEDGMENT

I would like to express my deep gratitude to the management and Department of Mathematics of SRM Institute of Science and Technology for giving me the opportunity to conduct this research under this university.

REFERENCES

[1] Choi, S.U., Eastman, J.A. (1995). Enhancing thermal conductivity of fluids with nanoparticles (No. ANL/MSD/CP-84938; CONF-951135-29). Argonne National Lab.(ANL), Argonne, IL (United States).

[2] Aaiza, G., Khan, I., Shafie, S. (2015). Energy transfer in mixed convection MHD flow of nanofluid containing different shapes of nanoparticles in a channel filled with saturated porous medium. Nanoscale Research Letters, 10(1): 1-14.

[3] Timofeeva, E.V., Routbort, J.L., Singh, D. (2009). Particle shape effects on thermophysical properties of alumina nanofluids. Journal of Applied Physics, 106(1): 014304. https://doi.org/10.1063/1.3155999

[4] Loganathan, P., Nirmal Chand, P., Ganesan, P. (2013). Radiation effects on an unsteady natural convective flow of a nanofluid past an infinite vertical plate. Nano, 8(01): 1350001. https://doi.org/10.1142/S179329201350001X

[5] Hatami, M., Ganji, D.D. (2014). Natural convection of sodium alginate (SA) non-newtonian nanofluid flow between two vertical flat plates by analytical and numerical methods. Case Studies in Thermal Engineering, 2: 14-22. https://doi.org/10.1016/j.csite.2013.11.001

[6] Hatami, M., Sheikholeslami, M., Ganji, D.D. (2014). Nanofluid flow and heat transfer in an asymmetric porous channel with expanding or contracting wall. Journal of Molecular Liquids, 195: 230-239. https://doi.org/10.1016/j.molliq.2014.02.024

[7] Prasad, K.V., Vajravelu, K., Vaidya, H., Van Gorder, R.A. (2017). MHD flow and heat transfer in a nanofluid over a slender elastic sheet with variable thickness. Results in Physics, 7: 1462-1474. https://doi.org/10.1016/j.rinp.2017.03.022

[8] Ganesh, N.V., Chamkha, A.J., Al-Mdallal, Q.M., Kameswaran, P.K. (2018). Magneto-marangoni nano-boundary layer flow of water and ethylene glycol based γ Al_2O_3 nanofluids with non-linear thermal radiation effects. Case Studies in Thermal Engineering, 12: 340-348. https://doi.org/10.1016/j.csite.2018.04.019

[9] Sheikholeslami, M., Ganji, D.D., Javed, M.Y., Ellahi, R. (2015). Effect of thermal radiation on magnetohydrodynamics nanofluid flow and heat transfer by means of two phase model. Journal of Magnetism and Magnetic Materials, 374: 36-43. https://doi.org/10.1016/j.jmmm.2014.08.021

[10] Khan, I., Khan, W.A. (2019). Effect of viscous dissipation on MHD water-Cu and EG-Cu nanofluids flowing through a porous medium: A comparative study of Stokes second problem. Journal of Thermal Analysis and Calorimetry, 135: 645-656. https://doi.org/10.1007/s10973-018-7459-5

[11] Cogley, A.C., Vincent, W.G., Gilles, S.E. (1968). Differential approximation for radiative transfer in a nongrey gas near equilibrium. Aiaa Journal, 6(3): 551-553. https://doi.org/10.2514/3.4538

[12] Abu-Nada, E., Chamkha, A.J. (2010). Effect of nanofluid variable properties on natural convection in enclosures filled with a CuO-EG-water nanofluid. International Journal of Thermal Sciences, 49(12): 2339-2352. https://doi.org/10.1016/j.ijthermalsci.2010.07.006

[13] Ratchagar, N.P., Balakrishnan, V., Vasanthakumari, R. (2018). Influence of hall current in the MHD oscillatory flow of nanofluid: Application to the blood flow. International Journal of Applied Engineering Research, 13(16): 12486-12493.

[14] Sabu, A.S., Mathew, A., Neethu, T.S., George, K.A. (2021). Statistical analysis of MHD convective ferro-nanofluid flow through an inclined channel with hall current, heat source and soret effect. Thermal Science and Engineering Progress, 22: 100816. https://doi.org/10.1016/j.tsep.2020.100816

[15] Iqbal, Z., Akbar, N.S., Azhar, E., Maraj, E.N. (2018). Performance of hybrid nanofluid (Cu-CuO/water) on MHD rotating transport in oscillating vertical channel inspired by Hall current and thermal radiation. Alexandria Engineering Journal, 57(3): 1943-1954. https://doi.org/10.1016/j.aej.2017.03.047

[16] Khan, S.U., Shehzad, S.A., Rauf, A., Ali, N. (2018). Mixed convection flow of couple stress nanofluid over oscillatory stretching sheet with heat absorption/generation effects. Results in Physics, 8: 1223-1231. https://doi.org/10.1016/j.rinp.2018.01.054

[17] Mahato, N., Banerjee, S.M., Jana, R.N., Das, S. (2020). MoS2-SiO2/EG hybrid nanofluid transport in a rotating channel under the influence of a strong magnetic dipole (Hall effect). Multidiscipline Modeling in Materials and Structures, 16(6): 1595-1616. https://doi.org/10.1108/MMMS-12-2019-0232

[18] Colla, L., Fedele, L., Scattolini, M., Bobbo, S. (2012). Water-based Fe_2O_3 nanofluid characterization: thermal conductivity and viscosity measurements and correlation. Advances in Mechanical Engineering, 4: 674947. https://doi.org/10.1155/2012/674947

[19] Makinde, O.D., Mhone, P.Y. (2005). Heat transfer to MHD oscillatory flow in a channel filled with porous medium. Romanian Journal of physics, 50(9/10): 931.

[20] Abbas, Z., Hussain, S., Rafiq, M.Y., Hasnain, J. (2020). Oscillatory slip flow of Fe_3O_4 and Al_2O_3 nanoparticles in a vertical porous channel using Darcy's law with thermal radiation. Heat Transfer, 49(6): 3228-3245. https://doi.org/10.1002/htj.21771

[21] Waqas, H., Farooq, U., Liu, D., Abid, M., Imran, M., Muhammad, T. (2022). Heat transfer analysis of hybrid nanofluid flow with thermal radiation through a stretching sheet: A comparative study. International Communications in Heat and Mass Transfer, 138: 106303. https://doi.org/10.1016/j.icheatmasstransfer.2022.106303

[22] Das, S.S., Satapathy, A., Das, J.K., Panda, J.P. (2009). Mass transfer effects on MHD flow and heat transfer past a vertical porous plate through a porous medium under oscillatory suction and heat source. International Journal of Heat and Mass Transfer, 52(25-26): 5962-5969. https://doi.org/10.1016/j.ijheatmasstransfer.2009.04.038

[23] Mishra, S.R., Dash, G.C., Acharya, M. (2013). Mass and heat transfer effect on MHD flow of a visco-elastic fluid through porous medium with oscillatory suction and heat source. International Journal of Heat and Mass Transfer, 57(2): 433-438. https://doi.org/10.1016/j.ijheatmasstransfer.2012.10.053

[24] Choudhury, R., Das, U.J. (2012). Heat transfer to MHD oscillatory viscoelastic flow in a channel filled with porous medium. Physics Research International, 2012. https://doi.org/10.1155/2012/879537

[25] Al-Khafajy, D.G. (2016). Effects of heat transfer on MHD oscillatory flow of Jeffrey fluid with variable viscosity through porous medium. Advances in Applied Science Research, 7(3): 179-186.

[26] Chand, K., Singh, K.D., Sharma, S. (2014). Heat transfer in MHD oscillatory flow of dusty fluid in a rotating porous vertical channel. Indian Journal of Pure and Applied Mathematics, 45(6): 819-835. https://doi.org/10.1007/s13226-014-0091-6

[27] Khudair, W.S., Al-Khafajy, D.G.S. (2018). Influence of heat transfer on magneto hydrodynamics oscillatory flow for williamson fluid through a porous medium. Iraqi Journal of science, 59(1B): 389-397. https://doi.org/10.24996/ijs.2018.59.1B.18

[28] Hamza, M.M., Isah, B.Y., Usman, H. (2011). Unsteady heat transfer to MHD oscillatory flow through a porous medium under slip condition. International Journal of Computer Applications, 33(4): 12-17.

[29] Narayana, P.S., Venkateswarlu, B., Devika, B. (2016). Chemical reaction and heat source effects on MHD oscillatory flow in an irregular channel. Ain Shams Engineering Journal, 7(4): 1079-1088. https://doi.org/10.1016/j.asej.2015.07.012

[30] Srinivasacharya, D., Mendu, U. (2014). Thermal radiation and chemical reaction effects on magnetohydrodynamic free convection heat and mass transfer in a micropolar fluid. Turkish Journal of Engineering and Environmental Sciences, 38(2): 184-196. https://doi:10.3906/muh-1209-3.

[31] Chaudhary, R.C., Jha, A.K. (2008). Effects of chemical reactions on MHD micropolar fluid flow past a vertical plate in slip-flow regime. Applied Mathematics and Mechanics, 29: 1179-1194. https://doi.org/10.1007/s10483-008-0907-x

[32] Hamilton, R.L., Crosser, O.K. (1962). Thermal conductivity of heterogeneous two-component systems. Industrial Engineering Chemistry Fundamentals, 1(3): 187-191. https://doi.org/10.1021/i160003a005

[33] Jafar, A.B., Shafie, S., Ullah, I. (2020). MHD radiative nanofluid flow induced by a nonlinear stretching sheet in a porous medium. Heliyon, 6(6): e04201. https://doi.org/10.1016/j.heliyon.2020.e04201

[34] Shoaib, M., Raja, M.A.Z., Sabir, M.T., Islam, S., Shah, Z., Kumam, P., Alrabaiah, H. (2020). Numerical investigation for rotating flow of MHD hybrid nanofluid with thermal radiation over a stretching sheet. Scientific Reports, 10(1): 18533. https://doi.org/10.1038/s41598-020-75254-8

[35] Misra, J.C., Shit, G.C., Chandra, S., Kundu, P.K. (2011). Hydromagnetic flow and heat transfer of a second-grade viscoelastic fluid in a channel with oscillatory stretching walls: application to the dynamics of blood flow. Journal of Engineering Mathematics, 69: 91-100. https://doi.org/10.1007/s10665-010-9376-x

[36] Pal, D., Biswas, S. (2017). Influence of chemical reaction and soret effect on mixed convective MHD oscillatory flow of casson fluid with thermal radiation and viscous dissipation. International Journal of Applied and Computational Mathematics, 3: 1897-1919. https://doi.org/10.1007/s40819-016-0215-2

[37] Pandey, A.K., Kumar, M. (2017). Chemical reaction and thermal radiation effects on a boundary layer flow of nanofluid over a wedge with viscous and Ohmic dissipation. Научно-технические ведомости Санкт-Петербургского государственного политехнического университета. Физико-математические науки, St. Petersburg Polytechnical University Journal: Physics and Mathematics, 10(4): 54-72. https://doi.org/10.1016/j.spjpm.2017.10.008

[38] Sedki, A.M. (2022). Effect of thermal radiation and chemical reaction on MHD mixed convective heat and mass transfer in nanofluid flow due to nonlinear stretching surface through porous medium. Results in Materials, 16: 100334. https://doi.org/10.1016/j.rinma.2022.100334

[39] Kataria, H.R., Patel, H.R. (2016). Radiation and chemical reaction effects on MHD Casson fluid flow past an oscillating vertical plate embedded in porous medium. Alexandria Engineering Journal, 55(1): 583-595. https://doi.org/10.1016/j.aej.2016.01.019

[40] Patel, H.R. (2022). Soret and heat generation effects on unsteady MHD casson fluid flow in porous medium. Waves in Random and Complex Media, 1-24. https://doi.org/10.1080/17455030.2022.2030500

[41] Sasikumar, J., Govindarjan, A. (2016). Effect of heat and mass transfer on MHD oscillatory flow with chemical reaction and slip conditions in asymmetric wavy channel. ARPN Journal of Engineering and Applied Sciences, 11: 1164-1170.

[42] Sasikumar, J., Gayathri, R., Govindarajan, A. (2018). Heat and mass transfer effects on MHD oscillatory flow

of a couple stress fluid in an asymmetric tapered channel. In IOP Conference Series: Materials Science and Engineering. IOP Publishing, 402(1): 012167. https://doi.org/10.1088/1757-899X/402/1/012167

[43] Pal, D., Biswas, S. (2016). Perturbation analysis of magnetohydrodynamics oscillatory flow on convective-radiative heat and mass transfer of micropolar fluid in a porous medium with chemical reaction. Engineering Science and Technology, an International Journal, 19(1): 444-462. https://doi.org/10.1016/j.jestch.2015.09.003

[44] Gupta, S., Kumar, D., Singh, J. (2019). Magnetohydrodynamic three-dimensional boundary layer flow and heat transfer of water-driven copper and alumina nanoparticles induced by convective conditions. International Journal of Modern Physics B, 33(26): 1950307. https://doi.org/10.1142/S0217979219503077

[45] Zeeshan, A., Ali, Z., Gorji, M.R., Hussain, F., Nadeem, S. (2020). Flow analysis of biconvective heat and mass transfer of two-dimensional couple stress fluid over a paraboloid of revolution. International Journal of Modern Physics B, 34(11): 2050110. https://doi.org/10.1142/S0217979220501106

[46] Modather, M., Rashad, A.M., Chamkha, A.J. (2009). An analytical study of MHD heat and mass transfer oscillatory flow of a micropolar fluid over a vertical permeable plate in a porous medium. Turkish Journal of Engineering and Environmental Sciences, 33(4): 245-258. https://do i:10.3906/muh-0906-31

[47] Prakash, O.M., Makinde, O.D., Kumar, D., Dwivedi, Y.K. (2015). Heat transfer to MHD oscillatory dusty fluid flow in a channel filled with a porous medium. Sadhana, 40: 1273-1282. https://doi.org/10.1007/s12046-015-0371-9

[48] Shit, G.C., Mandal, S. (2020). Entropy analysis on unsteady MHD flow of Casson nanofluid over a stretching vertical plate with thermal radiation effect. International Journal of Applied and Computational Mathematics, 6(1): 2. https://doi.org/10.1007/s40819-019-0754-4

[49] Rashidi, S., Dehghan, M., Ellahi, R., Riaz, M., Jamal-Abad, M.T. (2015). Study of stream wise transverse magnetic fluid flow with heat transfer around an obstacle embedded in a porous medium. Journal of Magnetism and Magnetic Materials, 378: 128-137. https://doi.org/10.1016/j.jmmm.2014.11.020

[50] Misra, J.C., Adhikary, S.D. (2016). MHD oscillatory channel flow, heat and mass transfer in a physiological fluid in presence of chemical reaction. Alexandria Engineering Journal, 55(1): 287-297. https://doi.org/10.1016/j.aej.2015.10.005

[51] Falade, J.A., Ukaegbu, J.C., Egere, A.C., Adesanya, S.O. (2017). MHD oscillatory flow through a porous channel saturated with porous medium. Alexandria Engineering Journal, 56(1): 147-152. https://doi.org/10.1016/j.aej.2016.09.016

NOMENCLATURE

a_1,b_1	Amplitudes of irregular channel
a, b	Empirical shape factor
B_0	Electromagnetic induction
$d_1 + d_2$	Width of channel
B_o	Magnetic field intensity
d	Mean half width of channel
Gr	Grashof number
Pe	Peclet number
u	Axial velocity [ms^{-1}]
K	Porous medium [m^2]
p	Dimensionless fluid pressure
q	Radiative heat flux [W/m^2]
$(c_p)_s$	Specific heat capacitance of solid nanoparticle [JK^{-1}]
$(c_p)_f$	Specific heat capacitance of base fluid [JK^{-1}]
t	Time [ms^{-1}]
w	wall condition
H_1,H_2	Channel walls [m]
h_1,h_2	Dimensionless channel walls
N	Thermal radiation parameter
Nu	Nusselt number

Greek symbols

α	Mean radiation absorption coefficient [Wm^{-1}]
ρ_f	Densities of base fluid [kg m^{-3}]
ρ_s	Densities of solid nanoparticle [kgm^{-3}]
ρ_{nf}	Density of nanofluid [kg m^{-3}]
μ_{nf}	Dynamic viscosity of Nf [g]
$(\rho\beta)_{nf}$	Thermal expansion of Nf [kg m^{-3}]
$(\rho c_p)_{nf}$	Heat capacitance of Nf [kg m^{-3}]
k_{nf}	Thermal conductivity [$W.m^{-1}K^{-1}$]
β_s	Volumetric coeff. of thermal expansion of nanoparticle[K^{-1}]
β_f	Volumetric coeff. of thermal expansion of base fluid [K^{-1}]
σ	Electrical conductivity [$\Omega^{-1}m^{-1}$]
ϕ	Volume fraction
θ	Fluid temperature
λ	Pressure gradient
τ	Shear Stress at the wall
ω	Frequency of the oscillation

Abbreviations

Nf	Nanofluid
EG	Ethylene glycol
MHD	Magnetohydrodynamic
Np	Nanoparticle
Cu	Copper
Ag	Silver
Au	Gold
Al_2O_3	Alumina